Experimental Results of Interferer Suppression with a Compact Antenna Array

A. Hornbostel[1], N. Basta[2], M. Sgammini[3], L. Kurz[4], S. I. Butt[5] and A. Dreher[6]

[1,2,3,6]German Aerospace Center (DLR), Germany,

[1]achim.hornbostel@dlr.de, [2]nikola.basta@dlr.de [3]matteo.sgammini@dlr.de,

[6]achim.dreher@dlr.de

[4] RWTH Aachen, Germany, kurz@eecs.rwth-aachen.de

[5]Ilmenau University of Technology, Germany, safwat-irteza.butt@tu-ilmenau.de

Abstract: Array antennas with digital beamforming provide a powerful method for interference suppression. In the project KOMPASSION a miniaturised 2x2 element array antenna with reduced element spacing and a surface, which is only one quarter of the surface of a conventional four element array antenna, was developed. Because of the lower element distance strong coupling effects appear which have to be taken into account. Different designs of the antenna were tested, among which one variant uses a decoupling and matching network (DMN). The project included also the development of a complete L1/E1- GNSS receiver for tracking and processing of the GNSS satellite signals. The performance of the receiver and the miniaturised antenna was investigated by field tests.

BIOGRAPHIES

A. Hornbostel holds a diploma degree in electrical engineering and a Ph.D. from the University of Hannover, Germany. He joined the German Aerospace Center (DLR) in 1989 and is currently head of a working group on algorithms and user terminals at the Institute of Communications and Navigation. His main activities are presently in interference mitigation, hardware simulation and receiver development. He is member of ION, EUROCAE WG62 'Galileo' and VDE/ITG section 7.5 'Wave Propagation'.

N. Basta graduated in 2008 with major in telecommunications at the School of Electrical Engineering at the University of Belgrade, Serbia. In the same year he joined the Antenna Group in the Navigation Department of the German Aerospace Center (DLR). His main interests are design and characterization of microstrip antenna systems for GNSS applications as well as time-domain analysis of antenna arrays.

M. Sgammini received the BEng degree in electrical engineering in 2005 from the University of Perugia. He joined the Institute of Communications and Navigation of the German Aerospace Center (DLR) in 2008. His field of research is interference detection and mitigation for global navigation satellite systems (GNSS).

L. Kurz received the diploma degree in electrical engineering from RWTH Aachen University in 2007. Since then he is working as a PhD student at the Chair of Electrical Engineering and Computer Systems at RWTH Aachen. His research interests are in the field of satellite navigation and digital signal processing.

S.-I. Butt, born in 1983, did his Bachelors in Electronics Engineering from Ghullam Ishaq Khan Institute (GIKI) of Technology in 2004. Soon after graduating, he joined Pakistan's research organization NESCOM, in the department of Radars & Communications as Assistant Manager. His area of work was mainly related to development of Ku-Band monopulse radar RF front end. Then, in

2006 he did his Masters in Wireless Systems at KTH Sweden with full scholarship from National University of Sciences and Technology (NUST), Pakistan. He returned to NUST after completing his Master studies, and joined as Lecturer in the College of Telecommunications Engineering. Since 2010, he is a Ph. D. candidate at the Department of RF and Microwaves at Ilmenau University of Technology, Germany. His research interests include Antenna designing, RF front end development, Compact antenna arrays, Microwave devices, estimation, detection and modulation in wireless systems particularly GNSS

A. Dreher received the Dipl.-Ing. (M.S.) degree from the Technische Universität Braunschweig, Germany, in 1983, and the Dr.-Ing. (Ph.D.) degree from FernUniversität, Hagen, Germany, in 1992, both in electrical engineering. From 1983 to 1985, he was a Development Engineer with Rohde & Schwarz GmbH, Munich, Germany. From 1985 to 1992, he was a Research Assistant, and from 1992 to 1997, he was a Senior Research Engineer with the Department of Electrical Engineering, FernUniversität. Since 1997, he has been with the Institute of Communications and Navigation, German Aerospace Center (DLR), Wessling, Germany, where he is currently Head of the Antenna Research Group. His current research interests include smart conformal antennas and microwave structures for satellite communications and navigation. He is Senior Member of IEEE and member of the VDE/ITG section 7.1 ‘Antennas’.

1 INTRODUCTION

Safety critical navigation with current and future satellite navigation systems, e.g. for transport of persons and goods in the railway, aviation, maritime and road transport sectors, requires besides accurate and reliable navigation high resilience against interference. These high requirements for interference mitigation are difficult to fulfil by state-of-the-art receivers with non-directional single element antennas. Therefore, the utilisation of array antennas together with suitable adaptive algorithms for interference suppression and adaptive digital beamforming is a promising and powerful alternative (Cuntz et al., 2008; Konovaltsev et al., 2007; Hornbostel et al. 2013).

For realisation of the desired properties of the array antenna a minimum number of radiator elements is required. In a conventional array the elements are spaced by approximately half a wavelength. Consequently, the size of such array is larger than a single element antenna. However, the size of the antenna is a main constraint in many applications. If the size of the array could be significantly reduced by smaller element spacing the possibilities for real application would increase. In particular, a compact array with small size would be very attractive for mobile platforms because aesthetic and functional requirements, like integration in the surface of the carrier structure could be easier satisfied.

Therefore, in the project KOMPASSION a compact array with only a quarter-wavelength element spacing was designed including the development of the complete receiver chain and algorithms for interference suppression and steering of beams to individual satellites by digital beamforming (Dreher et al., 2012). By utilisation of the concepts described in (Weber et al., 2006; Weber et al., 2007; Warnick K. F. and M. A. Jensen, 2007) the size of the array could be significantly reduced by smaller element spacing while the degrees of freedom for diversity and the fulfilment of signal-to-noise receiver requirements should be kept. One of the main challenges was the handling of the stronger coupling effects between the radiator elements due to the reduced spacing. The goal of the project was to demonstrate that also with a compact array a high level of interference suppression comparable with a larger conventional array can be achieved without significant loss of performance with respect to other receiver requirements like signal-to noise ratio and position accuracy. The performance of the compact array was investigated in field tests and compared with commercial single antenna receivers and a conventional array with half wavelengths spacing.

2 DESCRIPTION OF SYSTEM

2.1 General Design

In the context of miniaturisation of robust multi-antenna GNSS receivers, one of the main goals of this study was reducing the footprint of the analogue part of the unit. Two major steps can be distinguished: size reduction of the antenna array through smaller elements and shorter distance between them and full integration of the front end module onto a chip. Closely spaced antennas induce high levels of mutual coupling between channels. Different analogue and digital techniques must be applied in order to overcome the losses caused by the coupling. It is clear that the design of the array strongly determines the rest of the receiving chains.

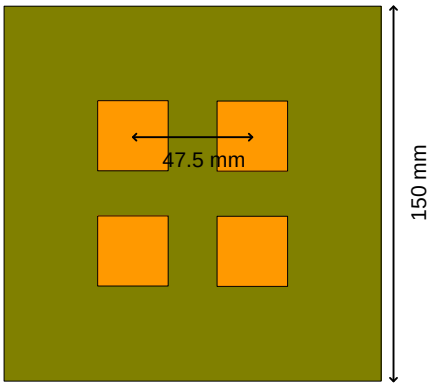

Figure 1. Antenna array of four elements

The developed antenna array contains four elements in a 2×2 square configuration whereas the footprint of the whole analogue unit is limited to a surface of 150×150 mm². The elements are based on microstrip technology and are miniaturised by using substrates of high dielectric constant (DK = 10.2). The embedded realised gain of the antenna element is 4 dBic. In general, four elements should allow enough degrees of freedom for simultaneous suppression of three interferers and thus robust reception in harsh conditions. However, these degrees of freedom are diminished due to the coupling. The overall system is dimensioned to a minimum of 4 MHz operation bandwidth at the central E1/L1 frequency 1.575 GHz. At this frequency, the smallest inter-element distance amounts to a quarter of the free-space wavelength (Figure 1).

In order to ensure the diversity and degrees of freedom of the coupled array, matching of the coupled array to the line impedance is required. Through a decoupling and matching network (DMN) optimal power transfer is enabled. The DMN is realised in two stages: Decoupling network (DN) and matching network (MN). The first stage performs orthogonalisation of the receiving patterns and, therefore, decouples the antenna ports. With low or no power flowing from one port to the other, standard matching techniques could be applied to the individual ports of the network. The orthogonal receiving signals coming out of the DMN are called modes.

The modes are fed into the front-ends where amplification, filtering and downconversion are performed. The front end is designed in 0.18-µm CMOS technology. The design enabled each of the four RF/IF paths (Figure 2) to be calibrated through a dedicated channel. An upconverted PRN calibration signal would be injected through couplers into the front ends, thus allowing online calibration of the phase and amplitude drifts in the electronic circuitry. A heterodyne architecture is employed, where the IF signals are sampled in bandpass. The digitised signals are then passed on to the processors on a FPGA board where the functionalities of beamforming, acquisition, tracking, DoA estimation and PVT estimation are implemented.

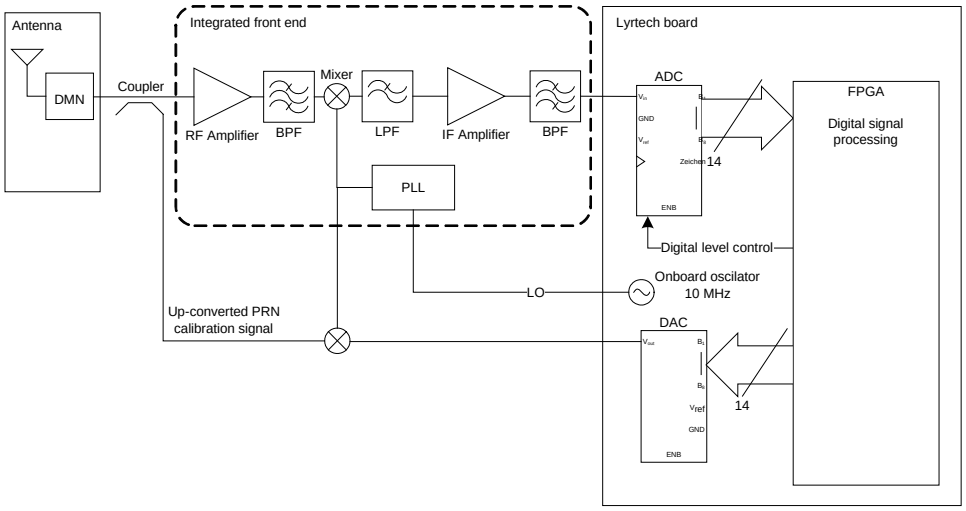

Figure 2. Block diagram of one channel of the system

2.2 Decoupling and Matching Network (DMN)

Besides the low radiation resistance of the higher-order modes, the reduction in the radiation efficiency of the higher-order modes of the compact antenna arrays is mainly associated with the reflection and dissipation power losses. The dissipation losses cannot be recovered. However, the reflection losses caused by the mutual coupling can be recuperated primarily by decoupling the antenna elements. Once decoupled, the antenna elements can be independently matched in order to transfer the entire available power between the antenna and receiver. The techniques to decouple the antenna elements can be divided into two major categories:

1. **Element-level decoupling**: Electromagnetic band-gap structures or parasitic elements between the radiating elements. This technique suffers from the narrow-band characteristics of the additional structures.
2. **Circuit-level decoupling**: Hybrid-couplers or the lumped components. This technique suffers from additional dissipation losses.

Here, we have implemented only circuit-level decoupling and matching network. We consider the implementation using 180^{o}-hybrid couplers, as we are mainly concerned with the benefits of such a DMN for compact antenna arrays designed for navigation applications.

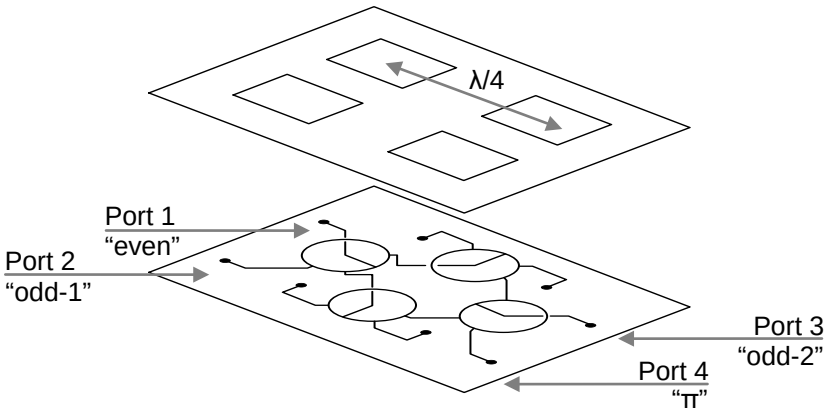

Figure 3. View of the integrated antenna array and DMN. Top: Antenna array. Bottom: Decoupling and matching network indicating the respective mode excitations.

The antenna array integrated with the DMN is shown in Figure 3. The antenna array comprises four elements in square geometry, with an inter-element separation of one quarter of the free-space wavelength. The measured mutual coupling coefficients exceed −10 dB, reaching a maximum of −8 dB without DMN. This causes the feed impedance of the antenna elements to vary for different directions-of-arrival, especially in the presence of nulls, which means reduced available carrier power due to mismatch power loss. The antenna array is symmetric; therefore, its eigenvectors correspond to the excitation vectors formed at the output of four 180-degrees hybrids if connected as shown in Figure 3. In addition to the decoupling of the antenna elements, tuning stubs provide matching of the individual modes. The DMN is designed using a dielectric substrate with relative dielectric permittivity of ε_r = 10.2 and a thickness of 1.27 mm. In order to minimize the losses between the network and the antenna feed-points, the outputs of the DMN are directly connected to the radiating elements using metallized vias. The detailed performance of the DMN is discussed in Irteza et al., 2013. As an example, with and without DMN co-polarized along with cross-polarized radiation patterns are shown in Figure 4.

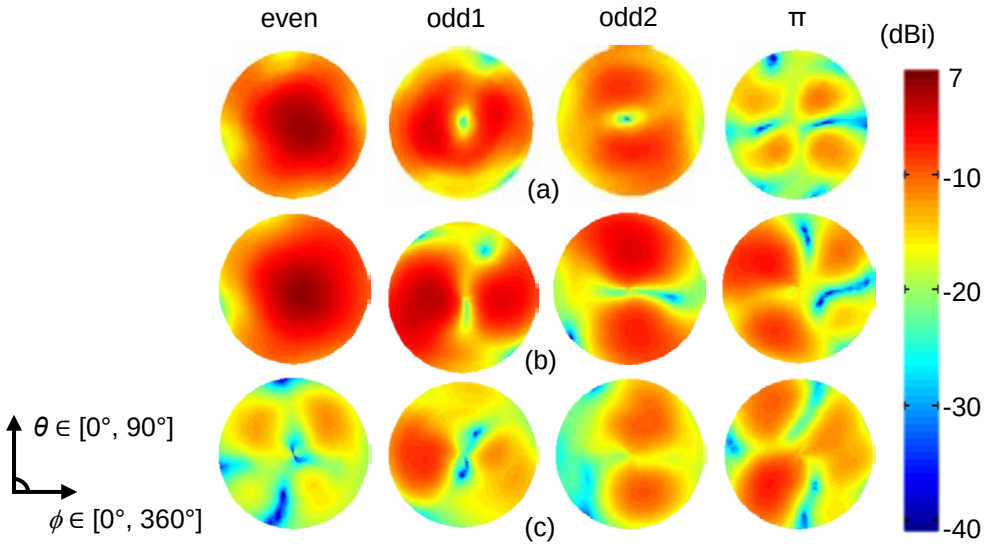

Figure 4. Realized gain radiation patterns of the compact array (polar colour-coded maps). (a) Ideal eigenmodes for the array excited with the exact eigenvectors with RHCP, without DMN. (b) Measured (RHCP) at the respective output ports of the DMN for the 1575.42 MHz. (c) Measured (LHCP) patterns with DMN.

2.3 Digital Receiver

The digital receiver is implemented on a hybrid prototyping platform which is composed of two FPGAs and a General Purpose Processor (GPP) (Cuntz et al., 2010). A block diagram of the digital platform is shown in Figure 5.

Signals from the analog frontend are sampled at high resolution (14 Bit) in order to allow undistorted processing of jamming signals. On FPGA#1 signals are filtered and down converted using cascaded decimation filters (DEC). Filters are implemented on a separate FPGA in order to save resources for baseband processing on the second FPGA. Data between the two FPGAs are transferred via the Xilinx RapidChannel interface.

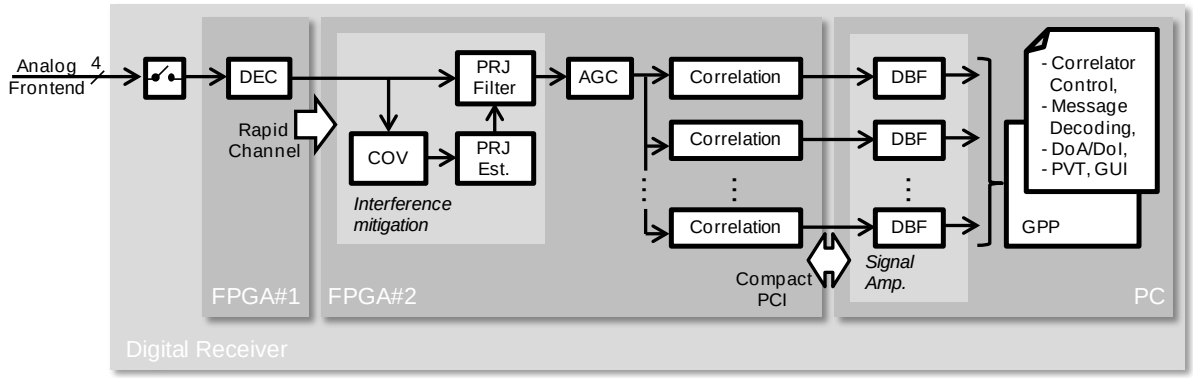

Figure 5. Scheme of digital unit and implemented functionalities

Prior to the correlation process, interference mitigation is applied in a dedicated filter which implements the first stage of the blind adaptive two-stage beamforming algorithm described in section 2.4. In Figure 5 interference mitigation is divided into the building blocks pre-correlation covariance matrix estimation (COV), projector estimation (PRJ est.) and filtering (PRJ filter). The building blocks “COV” and “PRJ filter” are implemented in hardware since signals are processed at sampling rates in MHz-range. However, studies (Sgammini et al., 2012; Cuntz et al., 2010) have shown that projector estimation (basically the eigendecomposition) can be processed at lower rates in kHz-range. Therefore, this task has been shifted to baseband processing in software.

At the output of the projection filter, interference signals are removed from the desired signal plus noise. This allows re-quantization of the interference-free signal to much lower wordlengths (2 Bit) for further processing in the correlator channels. Re-quantization is implemented using a digital Automatic Gain Control (AGC).

Afterwards, correlation is computed on the second FPGA which allows implementation of up to four memory-based correlator channels plus additional two Linear Feedback Shift Register (LFSR)-based modules. GPS L1 and Galileo E1b signals can be processed in memory-based modules and the LFSR-based modules can only be used for GPS L1 signals. In contrast to single antenna correlator modules, input signals from all array elements are correlated with the locally generated replica signal which increases effort in terms of FPGA resources by a factor of four in this case.

Periodically (i.e. each ms) correlator outputs as well as the pre-correlation covariance matrix and AGC states are provided to the PC using the compact PCI interface. Further baseband processing (i.e. correlator control, pre- and post-correlation beamforming) is computed on the PC. As a result of the baseband processing, control values for the correlator modules and projector matrices are provided to the FPGA#2 via the PCI interface in opposite transfer direction.

In addition to baseband processing, the PC computes PVT, estimates the directions of arrivals (DoA) of signals and interferers (DoI), and displays results in a GUI (Figure 6). A multi-threading implementation for the receiver is required on the Microsoft Windows operating system. This is necessary in order to divide tasks into real-time critical (baseband processing) and background tasks (PVT, DoA, GUI).

2.4 Algorithms

In this work the robust two-step blind adaptive beamformer proposed in Sgammini et al., 2012 has been used. The algorithm is able to mitigate radio frequency interference (RFI) adaptively. Usually

beamforming approaches require a precise knowledge of several parameters like the true antenna array response, the Direction-of-Arrival (DoA) of the LOS signal and/or non-LOS (NLOS) signals and other hardware biases. Due to the self-adaptive behaviour of the two-stage beamformer, neither the knowledge of the antenna array response nor the knowledge of the LOS and NLOS DoAs are necessary.

The algorithm is based on orthogonal projections and requires the estimation of the spatial covariance matrix before and after correlation. The suppression of RFI takes place at pre-correlation and requires the estimation of the interference subspace in order to construct the projector.

The projector onto the orthogonal interference subspace can be obtained as (Sgammini et al., 2012)

$$\mathbf{P}_I^{\perp} = \mathbf{U}_N \mathbf{U}_N^{\mathrm{H}} = \mathbf{I} - \mathbf{U}_I \mathbf{U}_I^{\mathrm{H}}, \tag{2.1}$$

where $\mathbf{U}_N \in \mathbb{C}^{M\times(M-I)}$ and $\mathbf{U}_I \in \mathbb{C}^{M\times I}$ are the estimation of the noise and the interference subspaces of the sample spatial covariance matrix estimation $\mathbf{R}_{xx}$, respectively. M is the number of antenna elements and I the dimension of the interference subspace.

The post-correlation eigenbeamforming which maximizes the ratio between the power of the desired LOS signal and the power of the undesired NLOS signal plus noise can be obtained as (Sgammini et al., 2012)

$$\mathbf{w}_{opt} = \mathbf{u}_d, \tag{2.2}$$

where $\mathbf{w}_{opt}$ is the optimum weight vector and $\mathbf{u}_d$ is the eigenvector associated to the dominant eigenvalue of the eigendecomposition of the post-correlation covariance matrix ($\mathbf{R}_{yy}$).

For monitoring purposes, the two-stage beamforming approach allows direction of arrival estimation for interferers (Direction-of-Interferer (DoI) estimation) and satellite signals (DoA estimation). The concept for DoA/DoI estimation applied here is based on the MUltiple Signal Identification and Classification (MUSIC) algorithm (Schmidt and Franks, 1986). In general, the MUSIC spectrum is defined by

$$S_{\mathrm{MUSIC}}(\phi,\vartheta) = \frac{\mathbf{a}^{\mathrm{H}}(\phi,\vartheta)\mathbf{a}(\phi,\vartheta)}{\mathbf{a}^{\mathrm{H}}(\phi,\vartheta)\mathbf{P}_S^{\perp}\mathbf{a}(\phi,\vartheta)} \tag{2.3}$$

with

$$\mathbf{P}_S^{\perp} = \mathbf{I} - \mathbf{U}_S \mathbf{U}_S^{\mathrm{H}}. \tag{2.4}$$

In this case $\mathbf{U}_S$ holds the eigenvectors spanning the signal subspace of K_S signals. Searching K_S maxima in this spectrum reveals the estimated directions for these signals.

In order to estimate DoI for multiple interferers, $\mathbf{P}_S^{\perp}$ in (2.3) has to be replaced by $\mathbf{P}_I^{\perp}$ as defined by (2.1). But instead of computing the common MUSIC spectrum, we define the DoI-spectrum

$$S_{\mathrm{DoI}}(\phi,\vartheta) = \frac{1}{\sqrt{S_{\mathrm{MUSIC}}(\phi,\vartheta)}} = \sqrt{\frac{\mathbf{a}^{\mathrm{H}}(\phi,\vartheta)\mathbf{P}_I^{\perp}\mathbf{a}(\phi,\vartheta)}{\mathbf{a}^{\mathrm{H}}(\phi,\vartheta)\mathbf{a}(\phi,\vartheta)}} = \frac{\left\|\mathbf{P}_I^{\perp}\mathbf{a}(\phi,\vartheta)\right\|}{\left|\mathbf{a}(\phi,\vartheta)\right|}. \tag{2.5}$$

Compared to the original MUSIC-spectrum extrema have the same location with respect to ϕ,ϑ but minima are of interest for DoI estimation since the inverse spectrum is considered. Furthermore, $S_{\mathrm{DoI}}(\phi,\vartheta)$ generates a smoother spectrum with a defined range of values $S(\phi,\vartheta)\in[0,1]\;\forall\,\phi,\vartheta$.

The spectrum for a scenario with three interferers is shown in Figure 6 on the left-hand side of the beampattern window. Minima are blue coloured and indicate the DoI of the interferers.

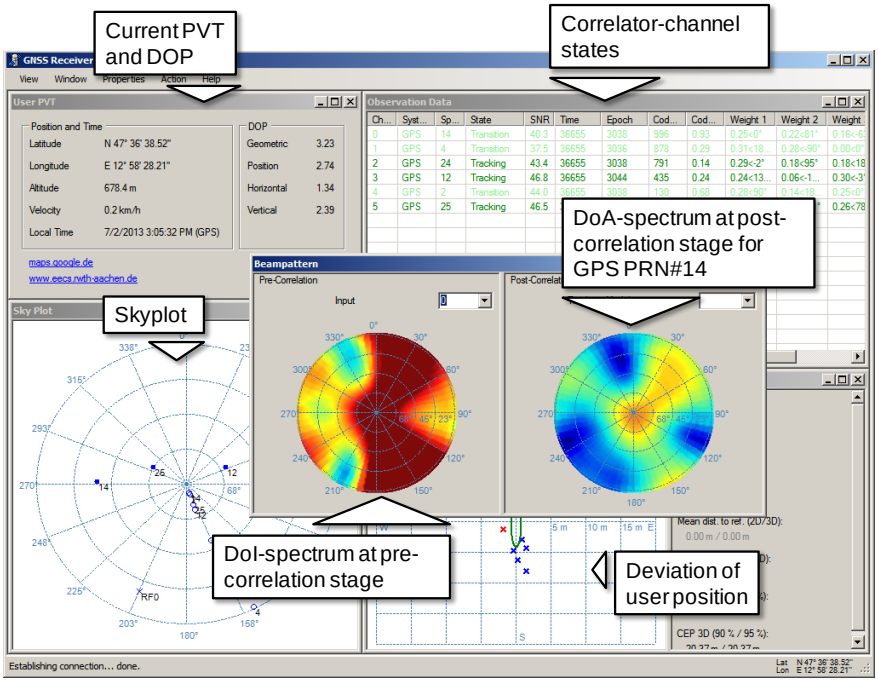

Figure 6. Graphical User Interface (GUI) in presence of three interferers

In case of DoA estimation in open-sky environments, the signal subspace is one-dimensional and unique for each satellite. Therefore, individual spectra have to be computed for each satellite and only the global maximum of (2.3) in each spectrum is of interest. It is obvious that

$$\begin{aligned}\arg\max_{\phi,\vartheta} S_{\text{MUSIC}}(\phi,\vartheta) &= \arg\max_{\phi,\vartheta} \frac{\mathbf{a}^{\text{H}}(\phi,\vartheta)\mathbf{a}(\phi,\vartheta)}{\mathbf{a}^{\text{H}}(\phi,\vartheta)\mathbf{P}_S^{\perp}\mathbf{a}(\phi,\vartheta)} \\ &= \arg\min_{\phi,\vartheta} \frac{\mathbf{a}^{\text{H}}(\phi,\vartheta)(\mathbf{I}-\mathbf{U}_S\mathbf{U}_S^{\text{H}})\mathbf{a}(\phi,\vartheta)}{\mathbf{a}^{\text{H}}(\phi,\vartheta)\mathbf{a}(\phi,\vartheta)} \\ &= \arg\max_{\phi,\vartheta} \frac{\mathbf{a}^{\text{H}}(\phi,\vartheta)\mathbf{U}_S\mathbf{U}_S^{\text{H}}\mathbf{a}(\phi,\vartheta)}{\mathbf{a}^{\text{H}}(\phi,\vartheta)\mathbf{a}(\phi,\vartheta)}\,. \end{aligned} \tag{2.6}$$

Therefore, by replacing $\mathbf{U}_S$ with the overall beamforming vector $\mathbf{P}_I^{\perp}\mathbf{w}_{opt}$ we can likewise identify DoA of satellite signals in the spectrum

$$S_{\text{DoA}}(\phi,\vartheta) = \frac{\left|\mathbf{w}_{opt}^{\text{H}}\mathbf{P}_I^{\perp}\mathbf{a}(\phi,\vartheta)\right|}{\left|\mathbf{a}(\phi,\vartheta)\right|} \tag{2.7}$$

which is the corresponding definition to (2.5). An example for the spectrum is shown in Figure 6 on the right-hand side of the beampattern window. The orange area close to the zenith indicates the DoA of the GPS satellite with PRN#14.

3 EXPERIMENTS

3.1 Static tests with three interferers

Static tests with 3 interferers were performed in the Galileo Test Environment (GATE) in Berchtesgaden. Figure 7 shows the test setup. CW-interferers were generated by signal generators and transmitted by two linearly polarized horn antennas and a circularly polarized patch antenna for interferer no. 2. During the tests the interference power was varied while the geometry was kept unchanged.

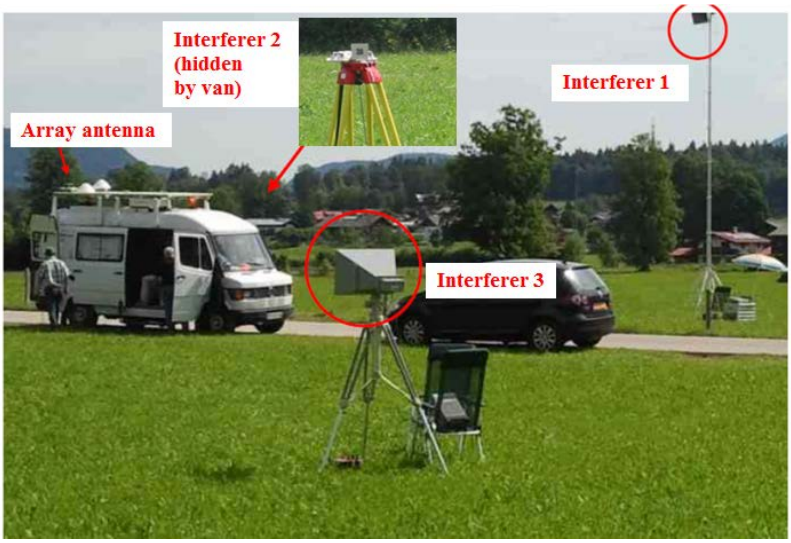

Figure 7. Experimental set-up with 3 interferers

Table 1 presents the interferer directions and distances relative to the position of the array receive antenna as well as the calculated jammer to signal ratio (J/S) for 0 dBm transmit power at the output of the signal generators and a nominal received satellite power of -125 dBm. Interferer 1 was transmitted at the GPS centre frequency. Interferers 2 and 3 had a frequency offset of +/-100 kHz. The J/S values include free space loss, gain of the transmit antennas and cable and polarization losses. The two horn antennas had a gain of 16.4 dB and the patch antenna (interferer 2) had a gain of 2.3 dB. Reference measurements with a third horn antenna confirmed that the calculations are accurate within a range of 2 to 3 dB.

Interferer no.	Frequency [MHZ]	Azimuth [°]	Elevation [°]	Distance [m]	Freespace loss [dB]	Gain and losses [dB]	J/S [dB]
1	1575.42	92.3	15.1	23.1	-63.7	11.6	72.9
2	1575.52	36.5	-3.5	22.3	-63.4	-3.7	57.9
3	1575.32	221.9	-3.3	22.4	-63.4	12.9	74.5

Table 1. Directions, distances and calculated J/S for 0 dBm transmit power

Measurements were performed with the miniaturised antenna (in the following called antenna A) with and without DMN and, for comparison, with a conventional array antenna with half wavelength spacing, which was developed in a previous project called GALANT. The antennas were connected to the KOMPASSION receiver, which used eigenbeamforming and another receiver which was developed also in the GALANT project and applies the minimum mean squared error approach for beamforming (Konovaltsev, 2007), (Litva, 1996). For further comparison, parallel measurements with a commercial high-end receiver and a commercial SW-receiver, which were connected to a commercial single element GPS-antenna were conducted.

Figure 5 shows the horizontal position error for single CW-interference by interferer 1. The interference power was increased versus time. The KOMPASSION receiver with miniaturised antenna and DMM provided a valid position for a J/S up to 68 dB, while the commercial high-end and the SW-

receiver, both with a single antenna, provided a valid position only up to J/S values of 48 dB and 33 dB.

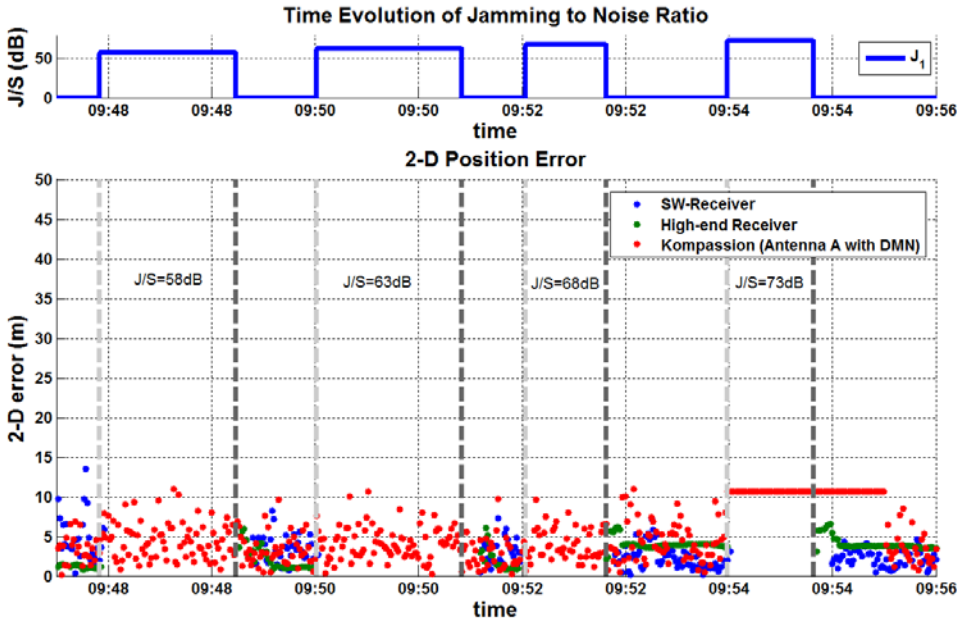

Figure 8. Horizontal position error with single CW-interferer

In Figure 9 two CW-interferers and additional PPD-interference (interferer 3) were switched on in parallel. The PPD-interference was generated by a commercial GPS-Jammer, a so-called privacy protection device (PPD), which was connected to the horn antenna of interferer 3. The PPD transmitted a chirp signal with constant power resulting in a J/S of 51 dB at the receive antenna. The power of the two CW-interferers was varied again. The maximum J/S of both CW-interferers, at which the KOMPASSION receiver with antenna A and DMN could still deliver a position was 33 dB, while the two commercial receivers lost the position already at the lowest generated J/S value of 23 dB.

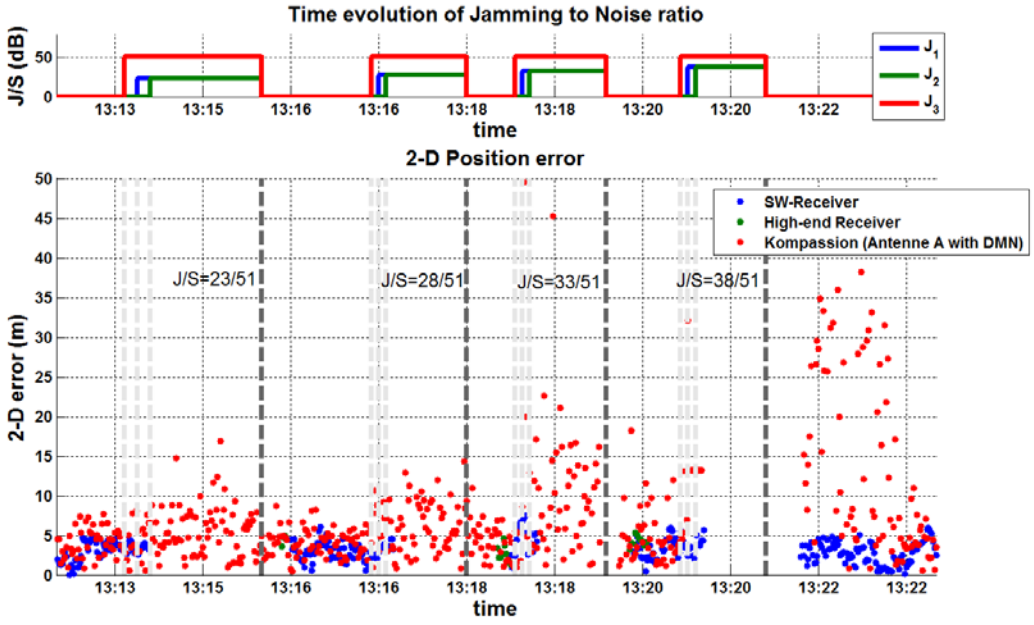

Figure 9. Horizontal position error with two CW-interferers and one PPD-interferer

Finally, in Figure 10, three CW-interferers were switched on one after the other until all 3 interferers transmitted simultaneously. In his case antenna A without DMN was used. Here, both the GALANT and the KOMPASSION receiver were connected in parallel to the antenna A without DMN. The KOMPASSION receiver delivered a position for two CW-interferers up to a J/S of 48 dB, but lost the position when the third interferer was switched on with same power. In contrast, the GALANT receiver still provides a position in this case. For two interferers the power could be further increased up to a J/S of 58 dB before the GALANT receiver lost its position (not shown in the figure). Probably, the recovery time was too short for the KOMPASSION receiver, before the next interference sequence was started. It is visible in the figure that it has still a large position error in the undisturbed case, before the first sequence with J/S = 53 dB starts. In the second attempt with same J/S it still delivers a position with two interferes, which shows, however, already a large error.

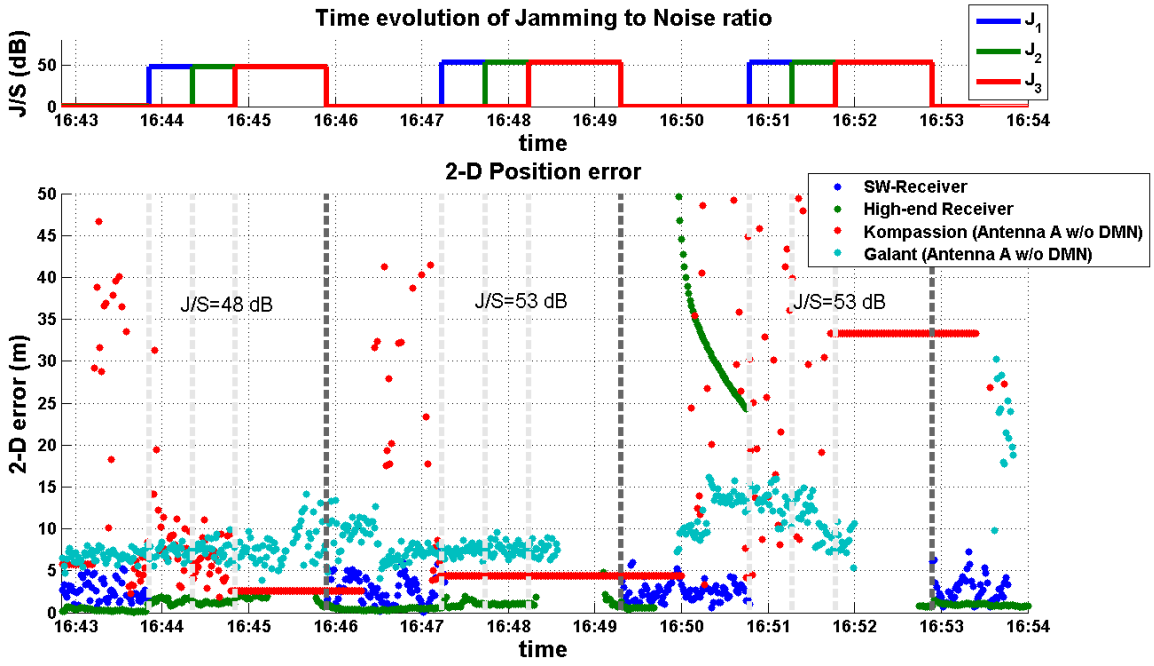

Figure 10. Horizontal position error with 3 CW-interferers

Table 2 presents a summary of the maximum achieved interferer suppression for the KOMPASSION receiver with different antennas. The last line shows, for comparison, the performance without interference mitigation by beamfoming (BF), i.e. when just a single element of the antenna was used. The values in brackets indicate that a position was still provided, but with significantly increased position error. For further comparison, Table 3 shows the maximum achieved J/S for the GALANT receiver with antenna A and for the two commercial receivers with a single element antenna. In the case of single CW-interference the KOMPASSION receiver shows the best results, while for 2 and 3 interferers the other receivers are partly better. However, the KOMPASSION receiver has only six parallel tracking channels due to limited FPGA resources, while the other receivers possess twelve or more parallel tracking channels, i.e. they can still provide a position if several satellites are already lost.

Antenna	1 CW	2 CW	2 CW + 1 PPD	3 CW
GALANT-Antenna	N/A	53	N/A	N/A
Antenna A	68	48 (53)	CW: 33, PPD: 51	23
Antenna A with DMN	68	33	CW: 33, PPD: 51	33
Antenna A with DMN without BF	48 (53)	N/A	N/A	N/A

Table 2. Maximum J/S in dB for which a position was still delivered by the KOMPASSION receiver

Receiver	1 CW	2 CW	2 CW + 1 PPD	3 CW
GALANT-receiver with antenna A	63	58	CW: 38, PPD: 51	48
High-end receiver	48 – 53	48 – 53	< 23	43
SW-receiver	33	23	< 23	23

Table 3. Maximum J/S in dB for which a position was still delivered other receivers

3.2 Dynamic tests

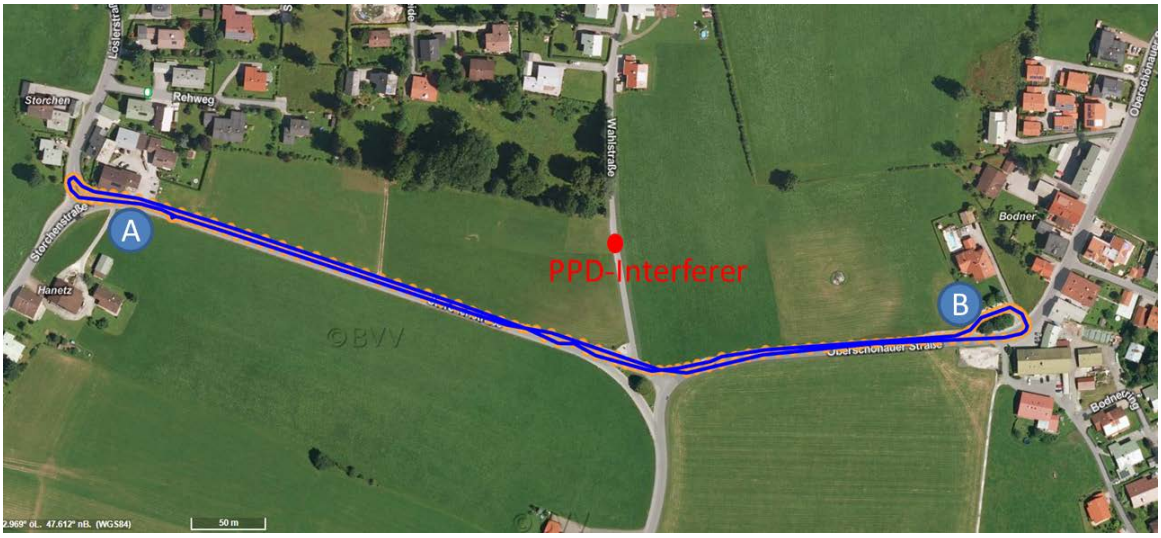

Figure 11. Scenario for dynamic test

A dynamic test was performed with a PPD jammer which was installed inside a car at a fixed position. The test receivers were installed in the measurement van, which started at point A in Figure 11, drove to point B and returned to Point A, i.e. it passed the jammer two times in a shortest distance of about 80 m. The jammer was switched on shortly before the measurements van started to move.

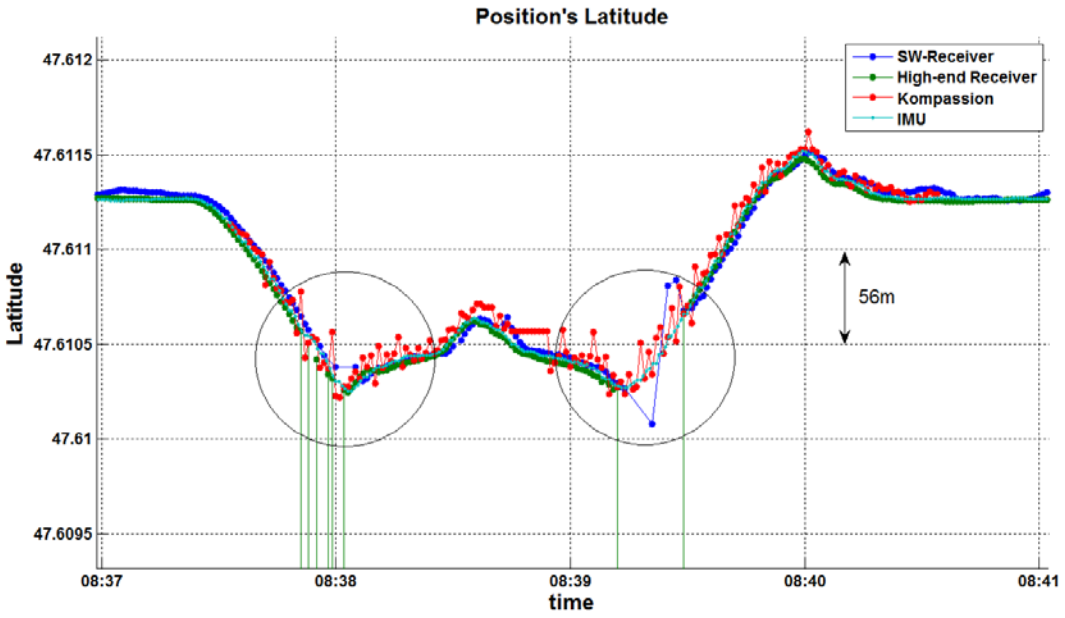

Figure 12. Latitude component of different receivers and IMU

Figure 12 shows the latitude position component measured by the different receivers and an inertial sensor (IMU) taken as reference. The two passages of the jammer are marked by circles. During both passages the commercial receivers had several outages, while the KOMPASSION receiver tracked continuously and was disturbed less. During the turn in point B also the KOMPASSION receiver lost the position. However, this was not due to the jammer, but probably due to shadowing. As mentioned before the KOMPASSION receiver has only 6 tracking channels, while the other receivers possess more channels, i.e. if three satellites are lost by shadowing, the KOMPASSION receiver loses the position, while the others can still provide a position.

4 CONCLUSIONS

An experimental receiver for robust satellite navigation with a compact antenna array and suitable algorithms for interference suppression has been developed and tested in the Galileo Test Environment (GATE) in Berchtesgaden. For this purpose, several scenarios with different jammers and receiver configurations have been arranged. It has been found that for single CW-interference the compact antenna with adaptive beamfoming provides 20 dB more robustness against interference than a conventional receiver with a single antenna. The advantage of the decoupling and matching network (DMN) becomes only visible in the case of three CW interferers. Also the commercial high-end receiver seems to have an interference mitigation method implemented which is effective for CW-interferers, although the spatial suppression by beamforming provides still some dB more robustness. However, in case of chirp signal interference caused by personal privacy devices (PPD) this method seems not to work and only the spatial methods with adaptive beamforming provide an effective means for interference suppression. So far as a comparison was possible from the experiments, there is no significant performance degradation with respect to interference suppression capability by the miniaturisation of the antenna compared to the classical array antenna with half wavelength spacing.

ACKNOWLEDGEMENTS

This work was funded by the Space Administration of the German Aerospace Center (DLR) on behalf of the Federal Ministry of Economics and Technology (FKZ: 50NA1006). The authors thank IFEN GmbH for their excellent support during conduction of the experiments in the GATE test bed.

REFERENCES

Cuntz M., H. Denks, A. Konovaltsev, A. Hornbostel, M. Heckler, F. Antreich, M. Meurer, and A. Dreher (2008). GNSS terminal concept and demonstrator with digital beamforming for future advanced applications in navigation, in proceedings of 30th ESA Antenna Workshop on Antennas for Earth Observation, Science, Telecommunication and Navigation Space Missions, Noordwijk, The Netherlands, May 2008, pp. 431-434.

Cuntz M., A. Konovaltsev, M. Heckler, M. Meurer, A. Hornbostel, A. Dreher, L. Kurz, G. Kappen, and T.G. Noll (2010**).** Lessons Learnt: The Development of a Robust Multi-Antenna GNSS Receiver, in proceedings of the 23rd International Technical Meeting of the Satellite Division of the Institute of Navigation ION GNSS, Portland, OR, USA, September 2010, pp. 2852–2859.

Dreher A. , N. Basta, S. Caizzone, G. Kappen, M. Sgammini, M. Meurer, S. Irteza, R. Stephan, M. A. Hein, E. Schäfer, M. A. Khan, A. Richter, B. Bieske, L. Kurz, and T.G. Noll (2012). Compact adaptive multi-antenna navigation receiver, in proceedings of ION GNSS, Nashville, TN, USA, Sept. 2012, pp. 917-925.

Hornbostel A., M. Cuntz, A. Konovaltsev, G. Kappen, C. Haettich, C.A. Mendes da Costa, and M. Meurer (2013). Detection and Suppression of PPD-Jammers and Spoofers with a GNSS Multi-Antenna Receiver: Experimental Analysis, in proceedings of ENC GNSS 2013, Wien, Austria.

Irteza S., E. Schaefer, M. Sgammini, R. Stephan, M. A. Hein (2013). Four-element compact planar antenna array for robust satellite navigation systems, in proceedings of 7th European Conference on Antennas and Propagation (EUCAP), 8-12 April 2013, pp.21-25.

Litva J. and T. Lo (1996). Digital Beamforming in Wireless Communications. Artech House.

Konovaltsev A., F. Antreich, and A. Hornbostel (2007)**.** Performance assessment of antenna array algorithms for multipath and interferers mitigation, in proceedings of 2nd Workshop on GNSS Signals & Signal Processing, Noordwijk, The Netherlands.

Kurz L., E. Tasdemir, D. Bornkessel, T.G. Noll, G. Kappen, F. Antreich, M. Sgammini, and M. Meurer (2012), An Architecture for an Embedded Antenna-Array Digital GNSS Receiver Using Subspace-Based Methods for Spatial Filtering, in proceedings of 6th ESA Workshop on Satellite Navigation Technologies NAVITEC 2012, pages 1–8, Noordwijk, The Netherlands.

Schmidt R. and R. Franks (1986). Multiple Source DF Signal Processing: An Experimental System. IEEE Transactions on Antennas and Propagation, vol. 34, no. 3, March 1986, pp. 281–290.

Sgammini M., F. Antreich, L. Kurz, M. Meurer, T.G. Noll (2012). Blind Adaptive Beamformer Based on Orthogonal Projections for GNSS, in proceedings of the 25th International Technical Meeting of the Satellite Division of the Institute of Navigation (ION GNSS 2012), Nashville, TN, September 2012, pp. 926-935.

Warnick K. F. and M. A. Jensen (2007). Optimal noise matching for mutually coupled arrays. IEEE Transactions on Antennas and Propagation, vol. 55, no. 6, June 2007, pp. 1726-1731.

Weber J., C. Volmer, K. Blau, R. Stephan, and M. A. Hein (2006). Implementation of a miniaturised antenna array with predefined orthogonal radiation patterns, in proceedings of EuCAP 2006, Nice, France.

Weber J., C. Volmer, K. Blau, R. Stephan, and M. A. Hein (2007), Miniaturized antenna arrays with an element separation down to $\lambda/10$. IEEE Antennas Propagat. Soc. Int. Symp. Dig., Honolulu, HI, June 2007, pp. 5897-5900.